Bioorganic & Medicinal Chemistry Letters 20 (2010) 726–729

Contents lists available at ScienceDirect

Bioorganic & Medicinal Chemistry Letters

journal homepage: www.elsevier.com/locate/bmcl

Isoxazolopyridone derivatives as allosteric metabotropic glutamate receptor 7 antagonists

Masayuki Nakamura *, Hideki Kurihara, Gentaroh Suzuki, Morihiro Mitsuya, Mitsuru Ohkubo, Hisashi Ohta

Banyu Tsukuba Research Institute, Banyu Pharmaceutical Co., Ltd, Okubo-3, Tsukuba, Ibaraki 300-2611, Japan

ARTICLE INFO

Article history:
Received 2 July 2009
Revised 10 October 2009
Accepted 13 November 2009
Available online 11 December 2009

Keywords:
mGluR7
Antagonist
Solid support synthesis
Isoxazolopyridone

ABSTRACT

This Letter describes the synthesis and evaluation of mGluR7 antagonists in the isoxazolopyridone series. In the course of modification in this class, novel solid support synthesis of the isoxazolopyridone scaffold was developed. Subsequent chemical modification led to the identification of several potent derivatives with improved physicochemical properties compared to a hit compound **1**. Among these, **2** showed good oral bioavailability and brain penetrability, suggesting that **2** may be useful for in vivo study to elucidate the role of mGluR7.

Metabotropic glutamate receptors (mGluRs) belong to a family of G protein-coupled receptors thought to contribute to the modulation of neuronal excitability and neurotransmitter release. Eight mGluR subtypes (mGluR1–mGluR8) have been cloned, and have been classified into three groups based on sequence homology, pharmacology and signal transduction pathway. Among these, mGluR7 is widely expressed in the central nervous system and the characteristics and functionality of mGluR7 have been extensively investigated.[1] As with several other members of the mGluR family, mGluR7 is primarily located on presynaptic terminals where it is thought to regulate neurotransmitter release.[1c,d] Of the presynaptic mGluR subtypes, however, mGluR7 is the most widely distributed and is present at a broad range of synapses that are postulated to be critical for both normal CNS function and a range of human disorders. Furthermore, unlike some presynaptic mGluR subtypes, mGluR7 is localized directly in the presynaptic zone of the synaptic cleft of glutamatergic synapses, where it is thought to act as a traditional autoreceptor that is activated by the glutamate released from the presynaptic terminal during action potentials. mGluR7 has been thought to be a key player in shaping synaptic responses at glutamatergic synapses as well as in regulating key aspects of inhibitory GABAergic transmission.[1d,e] However, mGluR7 has been the most intractable of the mGluR subtypes in terms of discovery of selective ligands.

Until the discovery of AMN082 **3** (Fig. 1), there have been no selective agonists or antagonists of this receptor[2] and it has been impossible to study the physiological effects of activation of this receptor without confounding effects induced by activation of these related mGluR subtype. Despite this lack of pharmacological tools, anatomical cellular studies, as well as experiments with mGluR7 KO mice, have led to suggestions that selective ligands for this receptor may treat a wide variety of neurological and psychiatric disorders.[3]

Mitsukawa reported the identification of AMN082 **3** with selective mGluR7 agonist activity, and found that the compound is orally active and penetrates the blood–brain barrier.[4] This pharmacological tool provided a breakthrough that may ultimately impact the understanding of the basic roles of mGluR7. Indeed, AMN082 **3** induced a robust increase in stress hormone levels that was absent in mGluR7 knockout animals, providing powerful support to a growing set of findings that suggest that antagonists of this receptor may be useful in conditions involving chronic stress such as depression and anxiety disorders.

Recently, we reported the discovery of novel mGluR7 antagonists and the comprehensive in vitro pharmacological characterization of isoxazolopyridone derivatives, such as **1** and **2** (Fig. 1).[5] In this study we showed that these isoxazolopyridone derivatives were allosteric mGluR7 antagonists and were selective against mGluR1, mGluR2, mGluR3, mGluR4, mGluR5, mGluR6, and mGluR8 at 1000 nM. However, only in vitro biological data were reported.

In this Letter, we describe the development of a novel solid support synthesis of the isoxazolopyridone derivatives which led to the discovery of potent and selective **2** with improved physicochemical properties. And we also report on the PK profile and brain penetrability of **2** in rats to determine if **2** could be useful for in vivo study.

* Corresponding author. Tel.: +81 29 865 4527; fax: +81 29 865 2170.
E-mail address: masayuki_nakamura2@oasis.ocn.ne.jp (M. Nakamura).

0960-894X/$ - see front matter © 2009 Elsevier Ltd. All rights reserved.
doi:10.1016/j.bmcl.2009.11.070

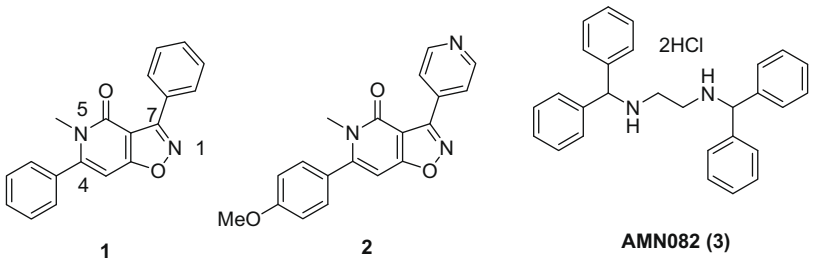

Figure 1.

After screening the in-house chemical collection, **1**, which contains an isoxazolopyridone scaffold, was identified as a hit compound. Compound **1** displayed mGluR7 antagonistic activity (IC_{50} = 20 nM) and had no detectable activity on other mGluRs at 1000 nM.[5] However, **1** showed poor metabolic stability (predicted F_H: 34%) on rat hepatocyte assay[6] and low aqueous solubility (0.17 μg/mL, pH 7.4).[7] We assumed that poor metabolic stability and low aqueous solubility may be due to its high lipophilicity (*c* log $D_{7.4}$: 3.5).[8] Therefore, our investigation of this class aimed to reduce the lipophilicity while retaining mGluR7 potency and to obtain tool compounds useful for in vivo study.

Structurally, **1** can be divided into three parts: the substitution on the *N*-5 position of the isoxazolopyridone core and the two aryl portions at the *C*-4 and *C*-7 positions. We envisioned that these three parts could be modified by introducing more hydrophilic substituents and/or replacing the aryl with heteroaromatic groups in order to reduce lipophilicity.

The synthetic route for the representative compound **2** is shown in Scheme 1. Condensation of 4-pyridinecarboxaldehyde **3** with hydroxylamine hydrochloride afforded oxime **4** in 94% yield. Oxime **4** was reacted with NCS in the presence of pyridine, followed by addition of ethyl 3-pyrrolidine-crotonate **5** to give isoxazole **6** in 60% yield, which was hydrolyzed to acid **7** in quantitative yield. Acid **7** was condensed with methylamine to give the corresponding amide **8** in 67% yield. Lithiation of amide **8** with excess *n*-BuLi at −78 °C followed by addition of methyl benzoate afforded the desired ketone **9** in 64% yield. Finally, cyclization of ketone **9** under acidic conditions gave the desired isoxazolopyridone derivative **2** in 60% yield. Other derivatives were synthesized in a similar manner, with slight modification of reaction conditions.[9]

Solid support synthesis is one of the most powerful tools in modern drug discovery to rapidly determine SAR data. Synthetically, as with the aryl portions on *C*-4, we attempted to develop a new solid support synthesis of the isoxazolopyridone scaffold. Taken the conventional synthesis shown in Scheme 1, we assumed that the amide NH in **8** would be connected to an appropriate resin and eventually released from under acidic conditions to facilitate spontaneous cyclization of the corresponding **9**, thereby providing the desired products. After optimization of reaction conditions, a solid support synthesis of the isoxazolopyridone around the aryl portions at *C*-4 was developed as shown in Scheme 2.

Reductive amination of commercially available ArgoGel-MB-CHO Resin™ **10** with methyl amine and $NaBH(OAc)_3$ gave methyl amine **11**, which was acylated with 5-methyl-3-phenylisoxazole-4-carboxylic acid using 2-chloro-1,3-dimethylimidazolium chloride. The resulting amide **12** was exposed to KHMDS in THF–toluene (1:1) at room temperature, followed by addition of commercially available esters[10] to afford ketone **13**. Finally, treatment with 50% TFA in CH_2Cl_2 furnished the desired derivatives, which were purified by silica gel chromatography or preparative HPLC.

The data for substituents on the *N*-5 and aryl portions at *C*-7 of the selected isoxazolopyridone derivatives are summarized in Table 1. Substitution with larger ethyl and *iso*-propyl groups on the *N*-5 position markedly decreased potency (**14** and **15**). In the series of the *C*-7 derivatives, the methoxy derivatives (**16, 17**, and **18**) have equipotent activity compared to **1** with retaining *c* log $D_{7.4}$ value. 4-Aza derivative **19** with reduced lipophilicity slightly decreased potency, while 3- and 2-aza derivatives (**20** and **21**) displayed 12-fold and >50-fold decreases in potency, respectively. Compound **19** also exhibited improvement of metabolic stability (predicted F_H: 65%) on rat hepatocyte assay. As expected, this result indicated that a decrease in lipophilicity was effective for

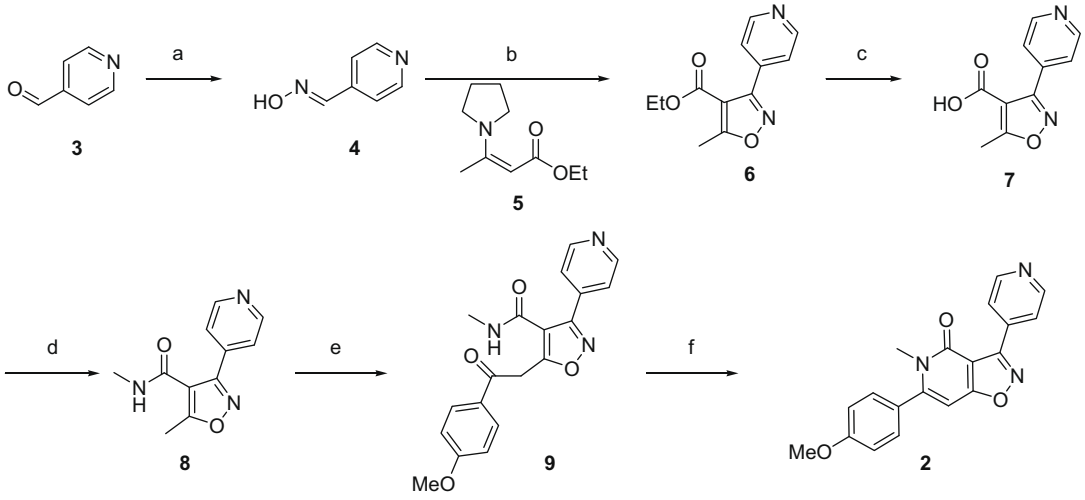

Scheme 1. Synthesis of isoxazolopyridone **2**. Reagents and conditions: (a) $NH_2OH{\cdot}HCl$, MeOH, reflux, 94%; (b) NCS, Py, $CHCl_3$, 50 °C, then **5**, Et_3N, 60%; (c) NaOHaq, MeOH, 100%; (d) $MeNH_2$, WSC, HOBt, DMF, rt, 67%; (e) *n*-BuLi, THF, -78 °C, then methyl 4-methoxybenzoate, 64%; (f) TsOH (cat.), toluene, reflux, 60%.

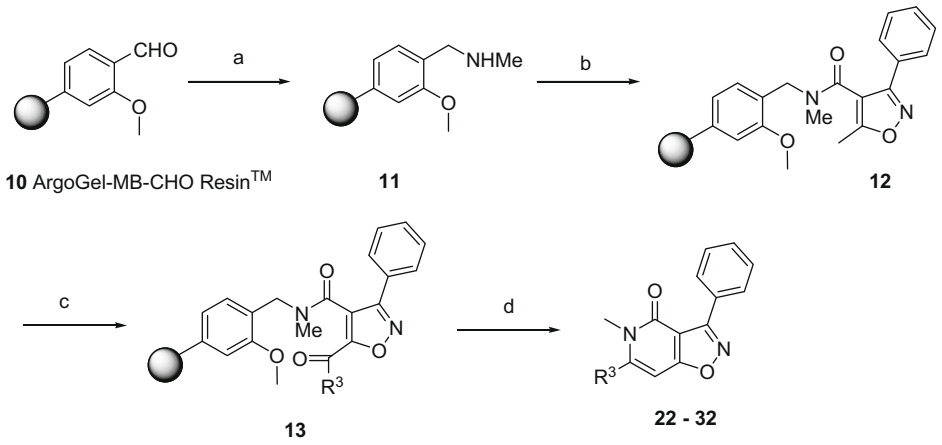

Scheme 2. Solid support synthesis of the isoxazolopyridone derivatives. Reagents and conditions: (a) $MeNH_2$, $NaBH(OAc)_3$, AcOH, DMF, rt; (b) 5-methyl-3-phenylisoxazole-4-carboxylic acid, 2-chloro-1,3-dimethylimidazolium chloride, *i*-Pr_2NEt, $CHCl_2$, rt; (c) KHMDS, THF, rt, then appropriate benzoate esters, rt; (d) TFA, CH_2Cl_2.

Table 1
SAR for isoxazolopyridone derivatives

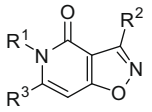

Compd	R^1	R^2	R^3	mGluR7 IC_{50}[a] (nM)	*c* log $D_{7.4}$	Metabolic stability predicted F_H (%)
1	Me	Ph	Ph	20	3.5	34
14	Et	Ph	Ph	910	3.9	
15	*i*-Pr	Ph	Ph	>10,000	4.5	
16	Me	4-MeO–Ph	Ph	29	3.6	
17	Me	3-MeO–Ph	Ph	12	3.6	
18	Me	2-MeO–Ph	Ph	21	3.6	
19	Me	4-Py	Ph	101	2.3	65
20	Me	3-Py	Ph	240	2.3	
21	Me	2-Py	Ph	1000	2.4	
22	Me	Ph	4-MeO–Ph	22	3.6	
23	Me	Ph	4-Me–Ph	51	4.0	
24	Me	Ph	4-F–Ph	72	3.8	
25	Me	Ph	4-Me_2N–Ph	140	3.6	50
26	Me	Ph	4-*i*-PrO–Ph	>10,000	4.2	
27	Me	Ph	4-*n*-Pr–Ph	150	4.9	
28	Me	Ph	3-Me_2N–Ph	31	3.6	
29	Me	Ph	3-CF_3–Ph	96	4.5	
30	Me	Ph	3,4-OCH_2O–Ph	26	3.5	
31	Me	Ph	3-F–4-MeO–Ph	210	3.7	
32	Me	Ph	3-Br–4-MeO–Ph	580	4.3	
2	Me	4-Py	4-MeO–Ph	26	2.4	76

[a] The IC_{50} values were calculated based on inhibition curves for 0.5 mM L-AP-induced Ca_2^+ mobilization in CHO cells expressing mGluR7 and Gα15 and were the mean of at least two independent assays.

improvement in metabolic stability in this class. Based on these results, 4-pyridine moiety was selected as an optimal substituent at the *C*-7 particularly due to its reduced lipophilicity.

SAR data for the *C*-4 aryl portion is also depicted in Table 1, although the information was very limited due to synthetic difficulty.[10] Generally, electron donating 4-methoxy, 3-dimethylamino and 3,4-methylenedioxy groups (**22**, **28**, and **30**) had tendency for maintaining mGluR7 potency. Compounds with larger substituents (**26** and **27**) and di-substituted compounds (**31** and **32**) were not acceptable, suggesting that bulkiness around the C-4 aryl portion was restricted.

Next, we combined the 4-pyridine group at the C-7 with the 4-methoxy at the C-4 based on the SAR above mentioned, providing compound **2**. As expected, **2** showed retained potency, reduced lipophilicity (*c* log $D_{7.4}$: 2.4) and improved metabolic stability (predicted F_H: 76%). And aqueous solubility (3.3 μg/mL, pH 7.4) was also improved compared to **1**.

In order to determine if **2** could be useful for in vivo study, we evaluated for PK profile[11] and brain permeability[12] in rats. The physicochemical and pharmacokinetic profiles of derivative **2** are given in Table 2. Compound **2** displayed good oral bioavailability with low plasma clearance in rats. We then examined brain penetrability (Table 3). Compound **2** was orally administrated to rats at 10 mg/kg. Plasma levels were then measured at 0.5 and 2 h after dosing, and brain penetrability (B/P) was also examined at 2 h post-dosing. The results showed that **2** had moderate plasma exposure and good brain penetrability.

In summary, synthesis and evaluation of a novel isoxazolopyridone class were performed. In the course of modification, novel solid support synthesis of this scaffold was developed. As a result, we

Table 2
Compared profiles of **1** and **2** and pharmacokinetic parameters in SD rats[a]

Compd	mGluR7 IC_{50} (nM)	$c\log D_{7.4}$	Solubility, pH 7.4 (μM/mL)	Predicted F_H (%)	F[b] (%)	AUC (μM h)	CLp[c] (mL/min/kg)
1	20	3.5	0.17	34	NT	NT	NT
2	26	2.4	3.3	76	65	0.71	1.0

NT, not tested.
[a] The values represent the mean for $n = 3$, iv (1 mg/kg) and po (3 mg/kg).
[b] Oral bioavailability.
[c] Plasma clearance.

Table 3
Brain penetration of **2**

Compound	Rat plasma (μM) level[a]		B/P ratio[b]
	0.5 h	2 h	
2	5.1	3.9	1.0

[a] Compound **2** (10 mg/kg) was orally administered to rats ($n = 3$), and the plasma levels were measured at 0.5 and 2 h.
[b] Compound **2** (10 mg/kg) was orally administered to rats ($n = 3$), and the plasma brain levels were measured at 2 h. B/P means the ratio of the brain level (nmol/g) to plasma level (μM) of **2**.

identified some isoxazolopyridone derivatives with potent mGluR7 antagonistic activity and metabolic stability compared to a hit compound **1**. Furthermore, **2** with improved physicochemical properties and metabolic stability showed good oral bioavailability and brain penetrability in rats. It is expected that **2** would be a good pharmacological tool for elucidating the role of mGluR7 on CNS functions in rodents and evaluation of **2** for efficacy in vivo will be reported in due course.

References and notes

1. (a) Okamoto, N.; Hori, S.; Akazawa, C.; Hayashi, Y.; Shigemoto, R.; Mizuno, N.; Nakanishi, S. *J. Biol. Chem.* **1994**, *269*, 1231; (b) Saugstad, J. A.; Kinzie, J. M.; Mulvihill, E. R.; Segerson, T. P.; Westbrook, G. L. *Mol. Pharmacol.* **1994**, *45*, 367; (c) Ohishi, H.; Nomura, S.; Ding, Y.-Q.; Shigemoto, R.; Wada, E.; Kinoshita, A.; Li, J.-L.; Neki, A.; Nakanishi, S.; Mizuno, N. *Neurosci. Lett.* **1995**, *202*, 85; (d) Kinoshita, A.; Shigemoto, R.; Ohishi, H.; van der Putten, H.; Mizuno, N. *J. Comp. Neurol.* **1998**, *393*, 332; (e) Kosinski, C. M.; Risso Bradley, S.; Conn, P. J.; Levey, A. I.; Landwehrmeyer, G. B.; Penney, J. B., Jr.; Young, A. B.; Standaert, D. G. *J. Comp. Neurol.* **1999**, *415*, 266; (f) Conn, P. J.; Niswender, C. M. *Proc. Natl. Acad. Sci. U.S.A.* **2006**, *103*, 251.
2. Yang, Z.-Q. *Curr. Top. Med. Chem.* **2005**, *5*, 913.
3. (a) Masugi, M.; Yokoi, M.; Shigemoto, R.; Muguruma, K.; Watanabe, Y.; Sansig, G.; van der Putten, H.; Nakanishi, S. *J. Neurosci.* **1999**, *19*, 955; (b) Sansig, G.; Bushell, T. J.; Clarke, V. R.; Rozov, A.; Burnashev, N.; Portet, C.; Gasparini, F.; Schmutz, M.; Klebs, K.; Shigemoto, R.; Flor, P. J.; Kuhn, R.; Knoepfel, T.; Schroeder, M.; Hampson, D. R.; Collett, V. J.; Zhang, C.; Duvoisin, R. M.; Collingridge, G. L.; van der Putten, H. *J. Neurosci.* **2001**, *21*, 8734; (c) Bough, K. J.; Mott, D. D.; Dingledine, R. J. *J. Neurophysiol.* **2004**, *92*, 1549; (d) Hölscher, C.; Schmid, S.; Pilz, P. K.; Sansig, G.; van der Putten, H.; Plappert, C. F. *Behav. Brain Res.* **2004**, *154*, 473; (e) Callaerts-Vegh, Z.; Beckers, T.; Ball, S. M.; Baeyens, F.; Callaerts, P. F.; Cryan, J. F.; Molnar, E.; D'Hooge, R. *J. Neurosci.* **2006**, *26*, 6573; (f) Mitsukawa, K.; Mombereau, C.; Lotscher, E.; Uzunov, D. P.; van der Putten, H.; Flor, P. J.; Cryan, J. F. *Neuropsychopharmacology* **2006**, *31*, 1112.
4. Mitsukawa, K.; Yamamoto, R.; Ofner, S.; Nozulak, J.; Pescott, O.; Lukic, S.; Stoehr, N.; Mombereau, C.; Kuhn, R.; McAllister, K. H.; Putten, H.; Cryan, J. F.; Flor, P. J. *Proc. Natl. Acad. Sci. U.S.A.* **2005**, *102*, 18712.
5. Suziki, G.; Tsukamoto, N.; Fushiki, H.; Kawagishi, A.; Nakamura, M.; Kurihara, H.; Mitsuya, M.; Ohkubo, M.; Ohta, H. *J. Pharmacol. Exp. Ther.* **2007**, *323*, 147.
6. The rank orders of predicted hepatic availability (F_H %) using rat hepatocytes: Shibata, Y.; Takahashi, H.; Ishii, Y. *Drug Metab. Dispos.* **2000**, *28*, 1518.
7. Yamashita, T.; Dohta, Y.; Nakamura, T.; Fukami, T. *J. Chromatogr.* **2008**, *1182*, 72.
8. Calculated $\log D_{7.4}$ values of compounds were expressed as $c\log D_{7.4}$ by utilizing PALLAS prologD, version 3.0, CompuDrug international Inc., CA, US.
9. Nakamura, M.; Kurihara, H.; Ohkubo, M.; Tsukamoto, N. PCT Application, WO02102807, 2002. Analytical data of compound **2**: ^{1}H NMR (300 MHz, $CDCl_3$) ppm: 3.45 (s, 3H), 3.90 (s, 3H), 6.56 (s, 1H), 7.03 (d, $J = 8.9$ Hz, 2H), 7.34 (d, $J = 8.9$ Hz, 2H), 8.30 (d, $J = 6.2$ Hz, 2H), 8.80 (d, $J = 6.2$ Hz, 2H). ESI-MS: m/z 334 $(M+1)^+$.
10. There was some limitation in this library. *ortho*-Substituted and pyridyl esters were unreactive, and the desired derivatives could not be obtained.
11. *Pharmacokinetics*. Pharmacokinetic characterizations were conducted in male SD rats following single oral and single intravenous administration. Single doses of **2** were administered intravenously in a vehicle of PEG400/EtOH/H_2O = 50:10:40 or orally by gavage in a vehicle of 0.5% methylcellulose aqueous suspension. Blood samples for the determination of drug plasma concentrations were obtained at multiple time points up to 8 h after administration. Blood samples were centrifuged to separate the plasma, and the plasma samples were deproteinized with ethanol containing an internal standard. Compound **2** and the internal standard were detected by LC–MS/MS in a positive ionization mode using the electrospray ionization probe, and the precursor to product ion combinations were monitored in multiple reaction monitoring mode.
12. *Plasma and brain concentrations in SD rats*. Compound **2** was suspended in 0.5% methylcellulose and orally administered to male Sprague-Dawley rats (7–10 weeks old, 200–400 g) at 10 mg/kg. At designated time after administration, blood was collected with a heparinized syringes from the abdominal aorta under isoflurane anesthesia. Then, the head skin was cut open, and a dental 30 G needle was inserted between the cervical vertebrae, and it was further inserted into the cavum subarachnoideale. After 50–100 μM cerebrospinal fluid had been collected by a 1 mL syringe through a tube connected to the needle, the brain was extracted. The blood sample was centrifuged (40 °C, 6000 rpm, 10 min) to separate plasma, and the plasma sample was deproteinized with threefold amount of ethanol containing an internal standard. The brain sample was homogenized with 2.0 mL of water by ultrasonification, and an aliquot of the homogenate was deproteinized with threefold amount of ethanol containing an internal standard. Theses samples were allowed to stand at −20 °C for 20 min and then centrifuged (4 °C, 12000*g*, 10 min). The supernatant was analyzed by LC–MS/MS, and the concentration of the test compounds in the plasma, brain, and cerebrospinal fluid were measured by the method using a relative calibration curve.